Annual Symposium of the Hellenic Nuclear Physics Society

Τόμ. 2 (1991)

HNPS1991

STUDY OF NUCLEON CORRELATIONS IN HEAVY NUCLEI WITH HIGH ENERGY ELASTIC ELECTRON SCATTERING

C. E. Vellidis, B. Frois, D. Goutte, N. Papadakis, C. N. Papanicolas, N. Vodinas, S. E. Williamson

doi: 10.12681/hnps.2843

STUDY OF NUCLEON CORRELATIONS IN HEAVY NUCLEI WITH HIGH ENERGY ELASTIC ELECTRON SCATTERING

C. E. VELLIDIS[1*], B. FROIS[2], D. GOUTTE[2], N. PAPADAKIS[1], C. N. PAPANICOLAS[1,3], N. VODINAS[1], S. E. WILLIAMSON[3]

[1] Athens University, Athens GREECE
[2] CEN-Saclay, Gif-sur-Yvette, FRANCE
[3] University of Illinois at Urbana-Champaign, Urbana, Illinois, USA

Abstract

During the last decade the detailed analysis of several observables and especially of electron scattering data has shown conclusively the presence of short-range nucleon correlations. As a result the degree to which the shape and amplitude of a correlated wave function can be approximated by an independent particle wave function has emerged as a question of fundamental importance. A presentation will be given below of an experiment that will be performed at the Bates Linear Accelerator Center attempting to study this question. The elastic cross-section ratios from $^{208,207,206}Pb,^{205}Tl(e,e)$ will be measured with high accuracy up to momentum transfers of 3.4 fm^{-1} in order to study the influence of correlations on the shape of the $3s_{1/2}$ proton wave function. The purpose, motivation and main aspects of the new research will be explained and the experimental considerations together with the running scenario for the experiment will be presented.

1. Introduction

During the last 25 years, electron scattering experiments from nuclei have provided one of the most precise tools for investigating nuclear structure. The electron, being a lepton, interacts weakly with the nucleus

* Presented by C. E. Vellidis

without absorption from it. It can penetrate the entire nuclear volume, giving information for the interior of the nucleus. The reaction mechanism between the electron and the nucleus is well understood in the framework of QED; as a result nuclear structure effects can be isolated from reaction effects with very high accuracy. Finally excellent beams of electrons with high energy and superb spatial and momentum resolution can be easily produced, due to recent technical developments in electron accelerator technology.

During the same period substantial progress has also been achieved in the nuclear many-body theory. Calculations using various Skyrme-type or finite-range effective interactions have been made, treating the characteristics of the nuclear many-body system beyond the shell-structure: the nucleon correlations and the pairing effect. These calculations reproduce with remarkable accuracy most of the observables of finite nuclei.

An important early result concerning this line of research was the demonstration of the validity of the concept of single-particle orbital in a dense medium like the nucleus by the accurate determination of the charge density difference of ^{206}Pb from ^{205}Tl with elastic electron scattering at momentum transfers up to ~3 fm^{-1} [1-3]. This provided a good supporting evidence for the approximate validity of the mean field theory. Going beyond the mean-field approximation, analysis of a wide range of observables has brought into focus the issue of the partial occupancy of the shell-model single-particle orbitals, particularly pronounced near the Fermi level. It has been argued that this effect is primarily the result of nucleon correlations [4-6]. Data of higher accuracy and at higher momentum transfers are expected to provide additional information on the influence of these correlations, particularly to issues concerning the shape of wave functions and charge distributions.

We report here the goals, strategy and running scenario of a new high-energy elastic electron scattering experiment [7], that will attempt to provide an accurate description of the correlated $3s_{1/2}$ proton state in terms of a single-particle wave function. The experiment has recently been approved by the Program Advisory Committee and it will be performed within the next two years at the Bates Linear Accelerator Center in the USA.

2. Motivation and purpose of the experiment

2a. The limitations of the mean-field theory

The basis of most of the present theoretical models for the description of the nuclear structure is the mean-field approximation. It asserts that the nucleons in a finite nucleus can be viewed as moving independently driven by a mean field. In order that the nuclear system may be stable, the mean field is assumed saturated in the ground state of the nucleus, the assumption being supported by the small experimental value of the nuclear compressibility.

This approximation has two limitations. The first one concerns the finite size of the nucleus. The absence of nucleons outside of the nucleus does not permit to complete the picture of a mean field at the nuclear surface, so the model can not describe correctly the states of the surface nucleons. The importance of this inadequacy decreases with increasing total number of nucleons and vanishes in the extreme limit of the infinite nuclear matter. The second limitation concerns the reliability of the assumption of independent motion of the nucleons inside the nucleus. The relative success of mean-field theory in the description of single-particle states is due to the fact that the low energy nucleons can not scatter from their states into already occupied ones, because of the exclusion principle. So their mutual interactions are suppressed by Pauli blocking. However this argument is only approximately valid. The time-energy uncertainty relation permits the more energetic nucleons to scatter into unoccupied states above the Fermi level for times limited by the uncertainty relation and the energy conservation. As a result these nucleons do not occupy their mean-field orbits all of the time. This is the origin of the concept of partial occupancy of the mean-field orbits. These short-lived quantum fluctuations are identified as multi-particle correlations beyond the mean-field predictions. The number of correlated particles is specified by the scattering process. Thus the mean-field approximation may be considered as the zeroth order contribution in an expansion in terms of multi-particle correlations. The purpose of the experiment is to study the effect of these correlations on the form of the correlated $3s_{1/2}$ proton wave function.

As it has been argued above, the correlations are essentially short-lived quantum fluctuations of their motions from the corresponding mean-field orbits. The removal of some nucleons to states above the Fermi level during some time intervals permits also the rearrangement of the remaining nucleons below the Fermi level in the same time intervals, due to scattering to the partially unoccupied states. Thus arises the necessity of a general modification in form of the mean-field single-particle wave functions, so as to account for the effect of all these quantum fluctuations [4,5]. This is what we shall study in particular for the 3s proton wave function. The origin of this problem lies on the fermion nature of nucleons. Thus it concerns all of the physics of Fermi liquids. From that general point of view it is hoped that the new experiment will provide information on a correlated single-particle wave function in a dense Fermi system.

2b. Quasi-particle orbits in Fermi liquids

It has been mentioned above that the shape and nature of single-particle orbits does not concern uniquely the nuclear physics. There exists an analogous problem for the orbits of the atoms in the atomic Fermi liquids. This analogy is expected because in an atomic Fermi liquid one has again a system of fermions interacting by some type of force (e.g. Van der Waals) assumed saturated, the assumption supported by the small compressibility of the liquid. As in atomic nuclei, one can outline an analogous mean-field picture for the liquid, with the corresponding limitations due to correlations of the atoms. In such a framework Lewart et al. [8] have investigated drops of atomic ^{3}He liquid. They have used variational Monte Carlo - Metropolis methods to study the wave functions of 20 - 240 atoms. The study of atomic droplets is easier than the study of nuclei because of the simplicity of the atomic interaction relative to the nuclear one, but the results illuminate aspects of the corresponding problems in nuclei.

In the many-body theory one can define single-particle wave functions in different ways by choosing to reproduce various observables of the many-body system [4,8,9,10]. Our interest is concentrated on the following two types of single-particle orbitals, included in the analysis of the above authors:

I. The ordinary mean-field model orbitals, defined so as to reproduce the density of the many-body system. Such orbitals can only be defined within a model, thus entering an overall systematic uncertainty to the analysis of all experimental results.

II. The "quasi-particle" orbitals, defined by the overlap integrals $\langle \Psi^{N+1} | \Psi^{N} \rangle$ for a quasi-particle and $\langle \Psi^{N-1} | \Psi^{N} \rangle$ for a quasi-hole, where $|\Psi^{N+1}\rangle$, $|\Psi^{N}\rangle$ and $|\Psi^{N-1}\rangle$ are the ground-state vectors of systems of N+1, N and N-1 particles respectively. In case of uncorrelated fermions, these vectors are simply the Slater determinants of the corresponding mean-field single-particle state vectors. The orbitals of this type are of particular interest because they can be defined in terms of physical observables, as it follows from their definition, and thus they have a meaning outside the domain of a given model.

Lewart et al have appropriately accounted for the effect of two- and three-body correlations on the single-particle orbitals using the corresponding correlation functions in the definitions of the variational ground-state total wave functions of the drops.

For our case the most important results are those concerning the drops of ^{3}He with N=70 and N=69 atoms, differing by an atom occupying the $3s_{1/2}$ state in the closed N=70 drop; that is, just like the nuclei of ^{206}Pb and ^{205}Tl which differ by a $3s_{1/2}$ proton. In Fig.1 we can make the comparison of these results with the corresponding ones for the nuclei. On the top the points of the Monte Carlo simulation for the density difference $r^2[\rho_{N=70}(r)-\rho_{N=69}(r)]$ are presented together with the theoretical curves for $r^2\chi^2(r)$ (dot-dashed curve) and $r^2\psi^2(r)$ (continuous curve). Here $\chi(r)$ is the 3s mean-field orbital and $\psi(r)$ the 3s quasi-particle orbital $\langle \Psi^{70} | \Psi^{69} \rangle$. The curve corresponding to the quasi-particle orbital lies much closer to the simulation points than the one corresponding to the mean-field orbital. This is due to the fact that the state vectors $|\Psi^{69}\rangle$ and $|\Psi^{70}\rangle$ defining $\psi(r)$ account for all the correlations of the atoms contained in the two drops while $\chi(r)$ accounts only for these correlations concerning the 3s atom that are predictable within the limits of the mean-field approximation. In the

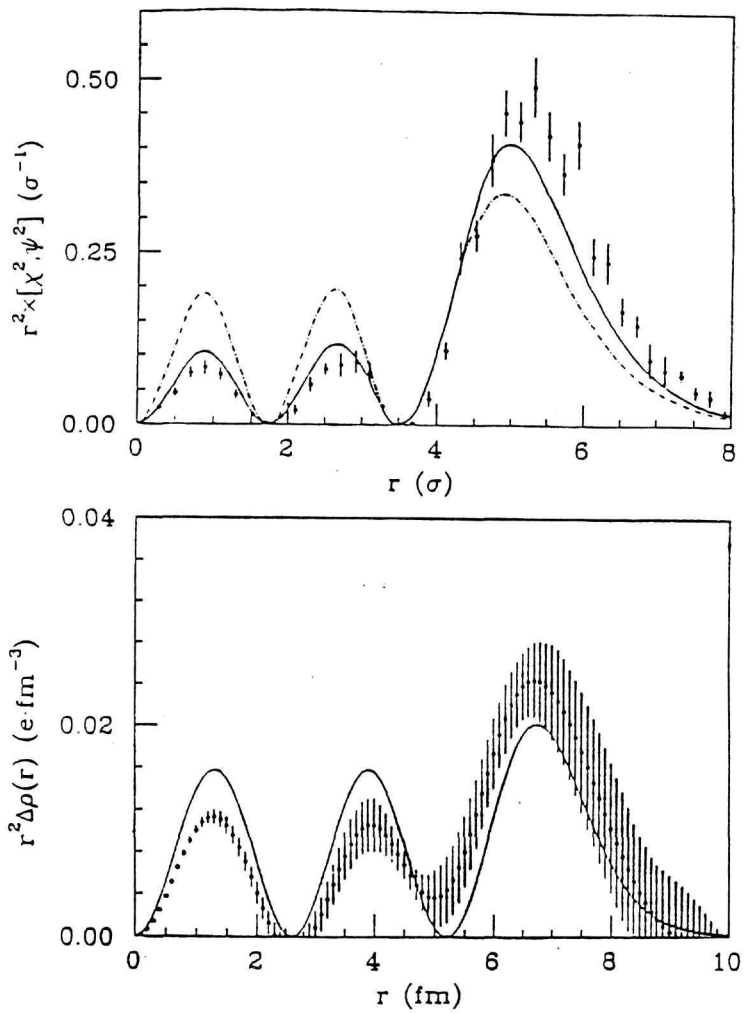

Fig.1 Top: atomic mean-field (dash-dotted curve) and quasi-particle (solid curve) wave function for liquid ^{3}He droplets. Density difference $\rho_{N=70}(r) - \rho_{N=69}(r)$ calculated by Monte-Carlo method (data points). **Bottom:** nuclear quasi-particle wave function inferred from the ^{206}Pb - ^{205}Tl charge density difference by removing the contribution of core polarization. The solid curve is a mean-field prediction for $\psi_{3s}(r)^2$.

bottom we may see the experimental points for $r^2[\rho_{206Pb}(r)-\rho_{205Tl}(r)]$ together with the theoretical curve for $r^2\psi^2_{proton}(r)$, where now $\psi_{proton}(r) = <\Psi^{82}|\Psi^{81}>$. The analogy between the results for the atomic and the nuclear systems suggests to study the nucleon correlations using the quasi-particle wave functions.

At this point it should be mentioned the general interest of this line of research for the physics of condensed matter. In a macroscopic dense medium the single-particle mean-field wave functions correspond to approximately infinite waves with a quasi-continuoum energy spectrum. Thus they are simply sines having frequencies that differ infinitesimally. Such wave functions are indiscernable. One needs a very small system of at most some hundreds of particles, stable in experimental conditions, with a discrete energy spectrum of the corresponding single-particle states, in order to discriminate a single-particle orbital. The atomic nuclei are such systems offered by Nature itself. They offer the possibility to observe with high precision a single-particle orbital in a dense medium.

3. The strategy of the new research

3a. Kinematical condition for the study of nucleon correlations

The ground state charge density provides detailed information on the wave function of the nucleus. High precision elastic electron scattering data measured to high momentum transfer are needed in order to reconstruct the nuclear charge density. The range of values of momentum transfer to which the cross section should be measured, in order to probe the influence of correlations, is specified by the fact that the correlated nucleons are scattered during a fraction of time into states above the Fermi level. For the protons in heavy nuclei the Fermi level corresponds to a Fermi momentum $k_F \sim 1.4$ fm^{-1}. In order to obtain information for protons occupying states above the Fermi level the momentum transfer must exceed the value $2k_F$ corresponding to the diameter of the Fermi sphere in momentum space. This value is the maximum momentum transfer that a nucleus could absorb without getting excited, if the states above the Fermi level were unoccupied during all of the time. At higher momentum transfer in the elastic scattering process we probe the partially occupied

states above the Fermi level and thus we obtain information for the correlated protons. We conclude that in order to study the proton correlations in heavy nuclei we need to measure elastic electron scattering cross sections to momentum transfers of the order or greater than 2.8 fm^{-1}.

The above estimation of the range of values of momentum transfer necessary for the study of nucleon correlations is confirmed experimentally. Fig.2 shows the percentage deviation of the mean-field elastic $^{208}Pb(e,e)$ total cross section from the experimental one, averaged over their sum, as a function of the effective momentum transfer q_{eff}. This quantity results from the ordinary momentum transfer after correction for the Coulomb attraction of the electron from the nucleus. The data shown in Fig.2 are taken from three different measurements at incident energies varying from 124 to 502 MeV, so the Coulomb correction to the momentum transfer varies from 12% to 3% respectively. The fraction of the difference of the total cross sections to their sum is multiplied by a factor of 200 for the sake of discrimination. One observes that the mean-field calculations predict very well the behavior of the cross section up to $q_{eff} \sim 2.3$ fm^{-1}. Data in this momentum transfer range are sensitive to the form of the nuclear surface and the average shape of the nuclear charge distribution. This follows from the relation of the resolving power of electron scattering Δr to the momentum transfer q (assuming that $h/2\pi = 1$):

$$\Delta r \sim \pi / q$$

resulting from the fact that the virtual photon exchanged between electron and nucleus is sensitive to electromagnetic field fluctuations of the order of its half wave length. At higher momentum transfers, that is for $q_{eff} \sim 3.0$ fm^{-1} (or $q \sim 2.8$ $fm^{-1} = 2k_F$) and beyond, a striking disagreement between experiment and theory appears. It is in this high momentum transfer region that elastic electron scattering data are sensitive to the details of the nuclear interior and that one obtains information on the correlated wave functions by observing their differences from the mean-field ones.

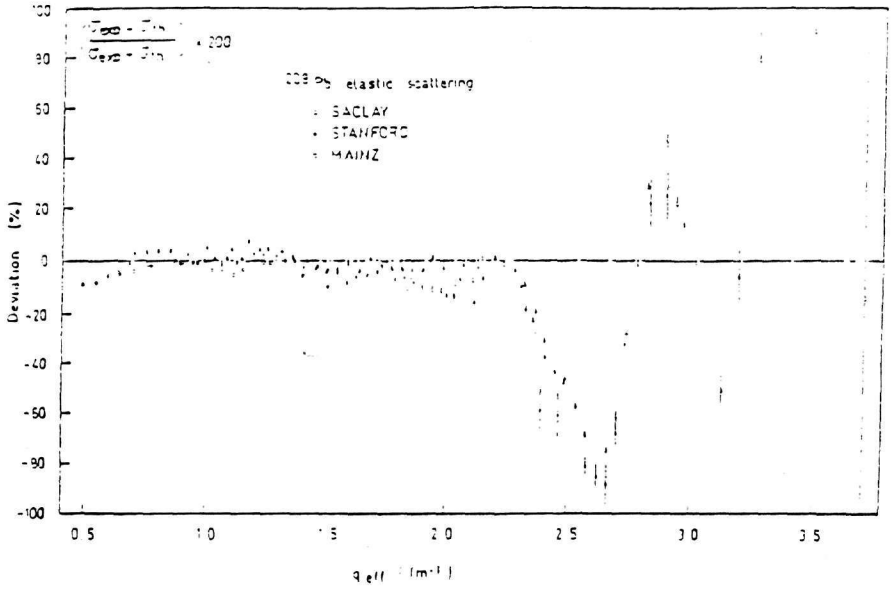

Fig.2 Deviation of the mean-field theoretical from the experimental ^{208}Pb(e,e) total cross section, normalized over their sum.

3b. The 3s proton orbital

In the experiment targets in the neighborhood of ^{208}Pb will be used. This choice is based on the fact that ^{208}Pb is the heaviest doubly closed nucleus. Consequently the description of nuclei in its neighborhood in terms of mean field theories is at the same time the simplest and the most exact one. These conditions ensure that the shell model is an accurate and also convenient starting point for the construction of single-particle orbitals. In Fig.3 the experimental points of the elastic ^{208}Pb(e,e) differential cross section $d\sigma/d\Omega$ as a function of the momentum transfer q, together with the corresponding mean-field (Hartree-Fock) prediction (dashed-curve) are shown. The discrepancies between experiment and theory are small and are visible only at high momentum transfers. The included diagram shows the ^{208}Pb charge density distribution $\rho(r)$ deduced from

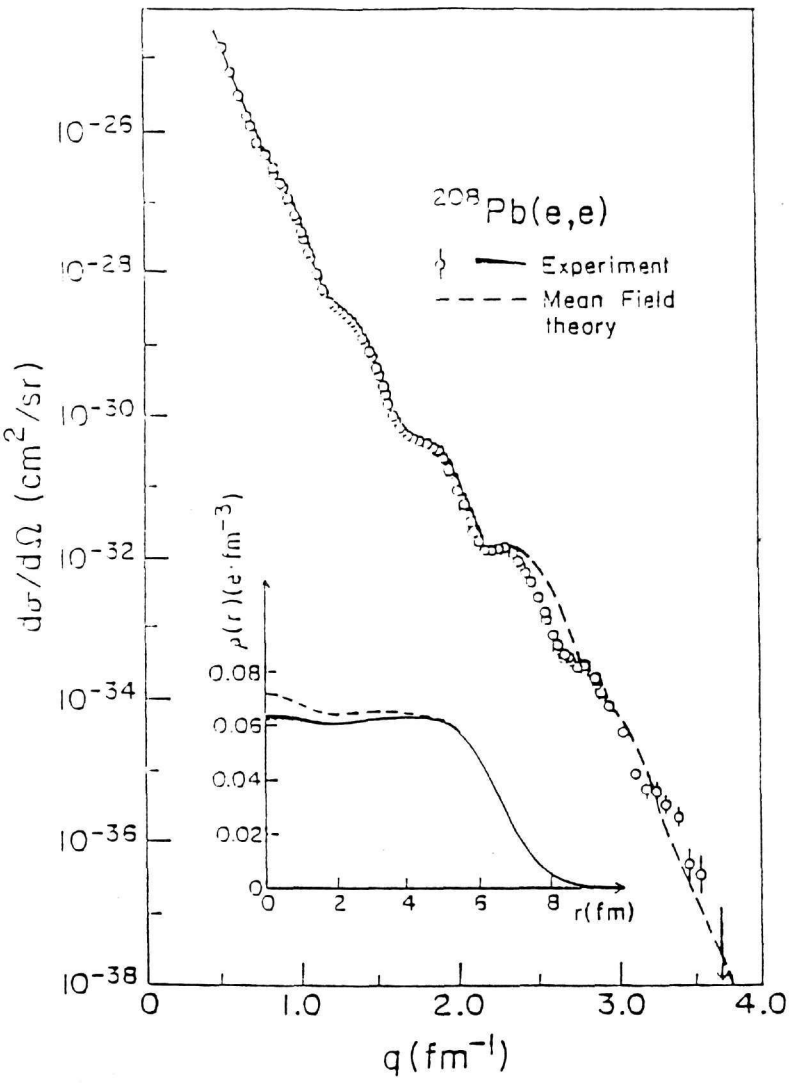

Fig.3 **^{208}Pb(e,e) experimental cross section (data points) and mean-field prediction (dashed curve). The included plot shows the ^{208}Pb charge density (solid curve) inferred from the data, together with the mean-field prediction. The thickness of the solid curve represents the experimental uncertainty.**

these points as a function of the radial distance from the center of the nucleus (continuous curve), together with the corresponding mean-field result (dashed curve). The experimental uncertainty is represented by the thickness of the continuous curve and increases with approaching the center of the nucleus. Here the discrepancy between experiment and theory is clear: the theory overestimates progressively the charge density as we approach the origin. This overestimation is due to the fact that the theory ignores the partial occupancy of the single-particle states which results to a redistribution of a fraction of the nuclear charge from the interior of the nucleus to the surface [6,11].

Using an electromagnetic probe like the electron to investigate the nuclear structure, we can obtain direct information mainly for the electrically charged protons (however it should be mentioned that for nuclei in the neighborhood of ^{208}Pb the contribution of the neutrons to the elastic electron scattering cross section is of the order of 30%). Thus we concentrate our attention to the proton states. In the Pb nucleus the highest-energy occupied level (valence level) is the $3s_{1/2}$, containing two protons. In the neighboring nucleus of Tl, this level contains only one proton. The experiment is directed to obtain information for the influence of correlations on the $3s_{1/2}$ proton orbital. The desired information will be achieved by measuring the ratio of the elastic electron differential cross sections $d\sigma(^{205}Tl)/d\sigma(^{206}Pb)$ in the range of momentum transfer $1.60\ fm^{-1} < q < 3.38\ fm^{-1}$, where the upper limit is the highest accessible value for this experiment. The reason for which ^{205}Tl has been chosen is that it is the stable isotope of Tl closer to the doubly magic ^{208}Pb (^{207}Tl would have been the obvious choice, but it is unstable). Consequently we need to study ^{206}Pb, which has the same core with an additional 3s proton as compared with ^{205}Tl. The 3s orbital has a very special shape with a unique and very narrow oscillatory behavior, peaked at r = 0, with two nodes at r = 2 fm and r = 4 fm (after unfolding from the finite proton size, see Fig.4). The 3s radial density with its three maxima and minima has then a damped oscillatory structure that has the largest overlap with the spherical Bessel function $j_0(qr)$ for $q \sim 2\ fm^{-1}$. Since the elastic electron scattering cross section is approximately proportional to the square of the charge form factor, which for a spherical nucleus is the Fourier-Bessel transform of the ground state charge distribution, the effect of the 3s proton will show up in the ^{205}Tl/^{206}Pb

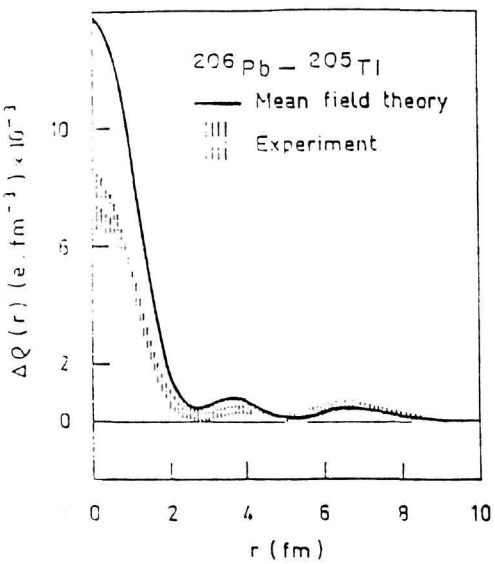

Fig.4 ^{206}Pb - ^{205}Tl charge density difference. The solid curve shows the mean-field prediction.

cross section ratio as a large peak, almost a $\delta(q-q_0)$ function, centered at q_0 ~2 fm^{-1}. The variation of the experimental cross section ratio of ^{205}Tl to ^{206}Pb as a function of the momentum transfer is shown in Fig.5. The very special shape of the 3s proton orbital produces a narrow structure at high momentum transfer and thus allows the unambiguous identification of the contribution of the 3s proton.

There exist several complications in the study of the ^{205}Tl/^{206}Pb cross section ratio. One comes from an effect known as the core polarization. The origin of it is that when some nucleons are removed from a nucleus the remaining ones should be redistributed in order to saturate the mean field of the nuclear forces in the space previously occupied by the removed nucleons. This redistribution results to a change in shape of the initial nucleus, from which the term "core polarization", producing consequently a total variation of the nuclear mean field. Thus the removal of some nucleons affects the orbits of the remaining ones in a complicated way and

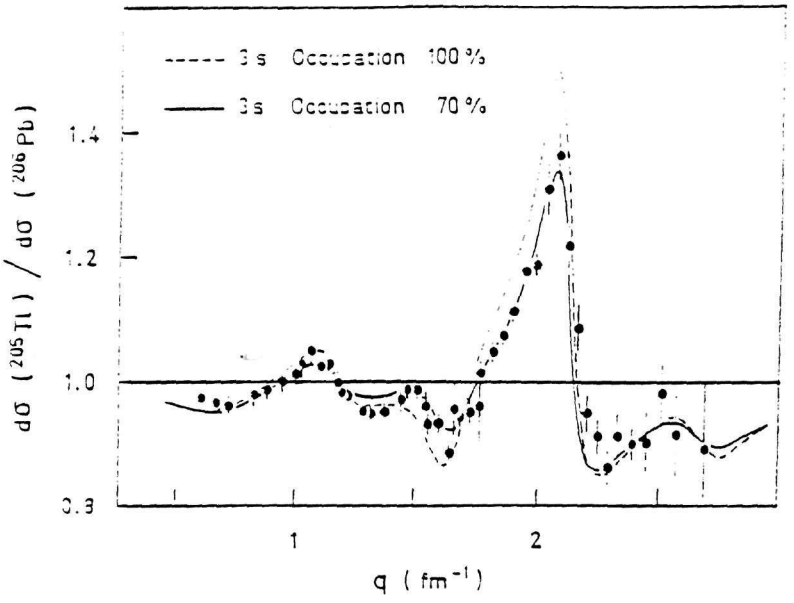

Fig.5 $^{205}Tl/^{206}Pb$ elastic electron cross section ratio (data points) and mean-field prediction. The solid curve shows the mean-field prediction with the strengths of the hole states $(3s_{1/2})_\pi^{-1}$ and $(2d_{3/2})_\pi^{-1}$ in Tl constrained to 0.7 and 0.3 respectively.

so has an important influence on the relation of scattering cross sections from two neighboring nuclei. However, since the core polarization due to neutron removal in ^{208}Pb is well described by theory [3], we can get direct information on the 3s proton orbital from the $^{205}Tl/^{206}Pb$ cross section ratio, with the aid of data on the cross section ratios $^{206}Pb/^{207}Pb$ and $^{207}Pb/^{208}Pb$. These ratios are more sensitive to core polarization effects because the nuclei $^{206,207,208}Pb$ have the same charge. So we can determine from them the amount of variations induced by core polarization due to neutron removal (after correction for the neutron form factor) and substract it from the total variations of the $^{205}Tl/^{206}Pb$ cross section ratio to get the clear effect of the 3s proton. Thus the elastic $^{207}Pb(e,e)$ and $^{208}Pb(e,e)$ differential cross sections should also be measured, in the same range of momentum

transfer as the ^{205}Tl(e,e) and ^{206}Pb(e,e) cross sections, so that we may study all the ratios $d\sigma(^{n}X)/d\sigma(^{n'}Y)$, where the symbols ^{n}X and $^{n'}Y$ stand for all the nuclei of ^{205}Tl and ^{206,207,208}Pb with n' = n+1.

Another complication may be observed in Fig.5. There the experimental data are compared to the predictions of density-dependent-Hartree-Fock (DDHF) calculations (dashed curve) which take into account some of the short-range correlations between nucleons, coming from the strong repulsive core of the nucleon-nucleon interaction . We observe that these calculations explain correctly the phase and shape of the oscillations of the cross section ratio, but they predict a significantly larger amplitude for the peak at 2.1 fm^{-1}. This discrepancy [2] can not be related to the influence of correlations, which appear at higher momentum transfer (see Fig.3). It can neither be related to the core polarization which, for the case of the nuclei ^{205}Tl and ^{206}Pb, corresponds mainly to a size decrease of ^{205}Tl with respect to ^{206}Pb, thus inducing appreciable variations at lower momentum transfer. In fact it is due to configuration mixing of the hole states $(3s_{1/2})_{\pi}^{-1}$ and $(2d_{3/2})_{\pi}^{-1}$ in Tl with respect to the magic Pb. A new DDHF calculation with the proton hole strength in Tl constrained to s_{3s} = 0.7 and s_{2d} = 0.3 gives the result shown in Fig.5 by the continuous curve, in excellent agreement with the experimental data. Configuration mixing in Tl affects the occupation probability of the 3s proton orbital [4] and it should be taken into account in the study of the ^{205}Tl/^{206}Pb cross section ratio. This is easy to do because this effect can be calculated starting from a mean-field basis.

3c. The search for the shape of the 3s proton orbital

From the above cross section ratios we can obtain information for the 3s proton orbital as a function of the momentum transfer, i.e. in the momentum space. To achieve information for the shape of that orbital, we need to transform the cross section data to the configuration space. This is a well known problem in nuclear physics [12-14]. This can be easily understood within the framework of the Plane Wave Born Approximation (PWBA). In PWBA the differential cross section of elastic electron scattering from a nucleus is proportional to the square of the modulus of the nuclear form factor; the proportionality factor represents simply the

cross section of scattering from a point-like target having the charge of the nucleus. This factor may be calculated exactly using QED. So we have direct information for (the modulus of) the form factor of the nucleus in momentum space. This quantity can be shown to be equal to the Fourier transform of the nuclear charge density distribution. The problem in applying the inverse transform to the configuration space is that the data for the form factor are always terminated at the maximum value q_{max} of momentum transfer accessible in the experiment, while the Fourier integration extends to infinite momentum transfers. Thus the direct reproduction of the charge density from the form factor is impossible. Instead one has to admit some model charge density distribution, for example an expansion in orthogonal functions truncated at the order corresponding to q_{max}, and to fit the deduced form factor to the one evaluated by the experiment. The fit determines the free parameters defining the model charge density; in case of an orthogonal expansion, the parameters are the coefficients of the terms. The model distribution should be chosen so as to introduce the least possible bias on the final result, a condition that holds for an orthogonal expansion. This condition gives rise to the characterization "model-independent" for the density determined in this way. However, by any means, the lack of knowlege for high momentum transfers introduces a completeness error to the final charge density; it must be combined with the statistical error due to the finite number of counts at each value of momentum transfer and the total error must be represented as a band of error bars in the final result. This may be achieved today by standard phase-shift-analysis methods using realistic estimations of the completeness errors. The propagation of the errors in the fitting procedure is calculated by standard error matrix techniques.

The error analysis is very important making reliable the conclusions deduced from the study of elastic electron scattering data. The corresponding result is shown in Fig.3 for the case of ^{208}Pb(e,e) data represented by the thickness of the continuous curve of the ^{208}Pb charge density distribution $\rho(r)$. As we may see in Figs.2 and 5, the uncertainty of the present elastic electron scattering data is large at high momentum transfers, where we should study the correlated 3s wave function. Because of the importance of the error analysis, among the purposes of the

experiment is to suppress the statistical uncertainty of the existing data in the high momentum transfer region.

In the shell-model the nuclear charge density distribution is just the sum of the squares of the proton single-particle wave functions folded by the finite size of the proton. Thus, after having determined the densities $\rho_{^{206}Pb}(r)$ and $\rho_{^{205}Tl}(r)$, their difference will be taken and unfolded from the proton size to get the 3s proton wave function together with the corresponding error band. Fig.4 shows the result derived from the existing data and also the mean-field prediction (continuous curve). We can see that experiment and theory agree in the phase of the three oscillations of (the square of) the wave function, but the theory overestimates the amplitude of the first two oscillations and underestimates that of the last one. This effect is more clear in the plot lying in the bottom of Fig.1, which is actually the same as Fig.5, apart from a factor of r^2 accounting for the radial dependence of a volume element containing a unit charge in the definition of the charge density. The disagreement between experiment and theory occurs because mean-field theory does not account for the partial occupancy of the 3s proton state, coming from correlations between nucleons and resulting to a partial redistribution of charge from the interior to the surface of the nucleus.

4. Experimental considerations and running scenario

In order to achieve the high momentum transfers and the high accuracy in measurements required for the experiment, several conditions should hold. First of all we need an electron beam with a large mean value of energy: $E_{beam} > 750$ MeV and with high energy and spatial resolution. A large value of average beam intensity: $I_{av} \sim$ 30-40 μA and a high beam luminosity are necessary for a high rate of counts even at large values of momentum transfer. The minimization of the highly enriched targets' thickness is necessary to reduce corrections of the data due to effects like bremmstrahlung, electron's self-interaction, multiple scattering and ionization losses. These corrections depend on the target thickness linearly or quadratically, as the corresponding effects occur inside or outside of the region of the primary scattering nucleus respectively. For the conditions holding the minimum effective range of the targets (assuming that they all

have approximately the same density) is ~70 mg/cm^2. There is also need for high momentum resolution in a broad range of momentum values of the scattered electrons. This may be achieved due to the momentum range and the excellent momentum resolution ($\delta p/p < 10^{-6}$) of the 1 GeV/c energy-loss magnetic spectrometer ELLSY of Bates. In addition we need a detecting system capable to measure extremely small values of differential cross sections. The existing detecting system at Bates has a limit of 10^{-40} cm^2/sr (or 10^{-16} b/sr) that exceeds the required range by almost two orders of magnitude. Finally we need a high-rate data acquisition system. All the above requirements are currently satisfied at the Bates Linear Accelerator facility.

Table I shows the running scenario for the experiment for 500 hours of beam. An incident energy of 750 MeV and an average beam current of 30 μA is assumed. In the first column the values of the momentum transfer q are listed in order of magnitude. The momentum transfer will be varied by keeping the incident energy E constant and by varying the scattering angle θ, as implied by the kinematical relation $q = 2E\sin(\theta/2)$, after neglecting the electron mass. The second column contains the number of counts at each value of q and the third column the corresponding percentage statistical errors. Finally the fourth column contains the cost in time for each measurement, estimated with a phase-shift calculation using theoretical densities. These densities are determined using the D1 force of Decharge and Gogny [15] (a phenomenological density-dependent finite-range force). A four hour overhead is assumed for every angle change. Up to $q = 3$ fm^{-1} the already existing ^{208}Pb(e,e) data, being sufficiently accurate, will be used. For $q > 3$ fm^{-1} we shall measure the ^{208}Pb(e,e) cross section to reduce the rather large statistical uncertainty in the data for our normalization nucleus.

Fig.6 shows the positions of the measurements with the corresponding statistical error bars on the axis of the effective momentum transfer q_{eff}. The included diagram shows the time needed to complete each measurement. There are also plotted the curves for $d\sigma(^{205}Tl)/d\sigma(^{206}Pb)$ resulting from four different calculations: a calculation using densities determined by extrapolation of a sum-of-gaussians (SOG) fit (continuous curve), which is a model-independent method of determination of nuclear charge densities from experimental data; a density-dependent Hartree-

TABLE I: Running scenario for the experiment

Targets	q(fm^{-1})	N° Counts	Error(%)	Time(hrs)
Calibrations	1.60			24.0
^{205}Tl,^{206,207}Pb	1.60	10000	1.3	1.0
^{205}Tl,^{206,207}Pb	1.70	10000	1.3	4.0
^{205}Tl,^{206,207}Pb	1.90	10000	1.3	4.0
^{205}Tl,^{206,207}Pb	2.00	10000	1.3	4.0
^{205}Tl,^{206,207}Pb	2.08	10000	1.3	4.1
^{205}Tl,^{206,207}Pb	2.14	10000	1.3	4.2
^{205}Tl,^{206,207}Pb	2.20	10000	1.3	5.0
^{205}Tl,^{206,207}Pb	2.31	10000	1.3	5.0
^{205}Tl,^{206,207}Pb	2.42	10000	1.3	5.5
^{205}Tl,^{206,207}Pb	2.53	10000	1.3	9.5
^{205}Tl,^{206,207}Pb	2.64	4000	2.3	11.0
^{205}Tl,^{206,207}Pb	2.78	4000	2.3	32.0
^{205}Tl,^{206,207}Pb	2.93	3000	2.6	49.0
^{205}Tl,^{206,208}Pb	3.08	1200	4.1	100.0
^{205}Tl,^{206,208}Pb	3.23	560	6.0	117.5
^{205}Tl,^{206,208}Pb	3.38	290	8.4	119.1

Fock plus BCS (HF+BCS) calculation with the effective Skyrme interaction (dot-dashed curve), accounting for the pairing effect and some of the short-range correlations; a Lipkin-Nogami (LN) calculation (dashed curve) which amounts to a variation of the HF+BCS states after approximate projection on the number of particles, thus enhancing the pairing correlations; and a Hartree-Fock-Bogolyubov (HFB) calculation using the realistic D1 force (dotted curve) [13-16]. The last calculation considers pairing, short-range and long range correlations within the limits of the mean-field approximation. We may observe that the high-q_{eff} measurements are the most expensive in time, inducing also large statistical errors; but they are the most important, because they penetrate the region where all the above calculations deviate strongly from the ideal value about 0.86 of the cross section ratio.

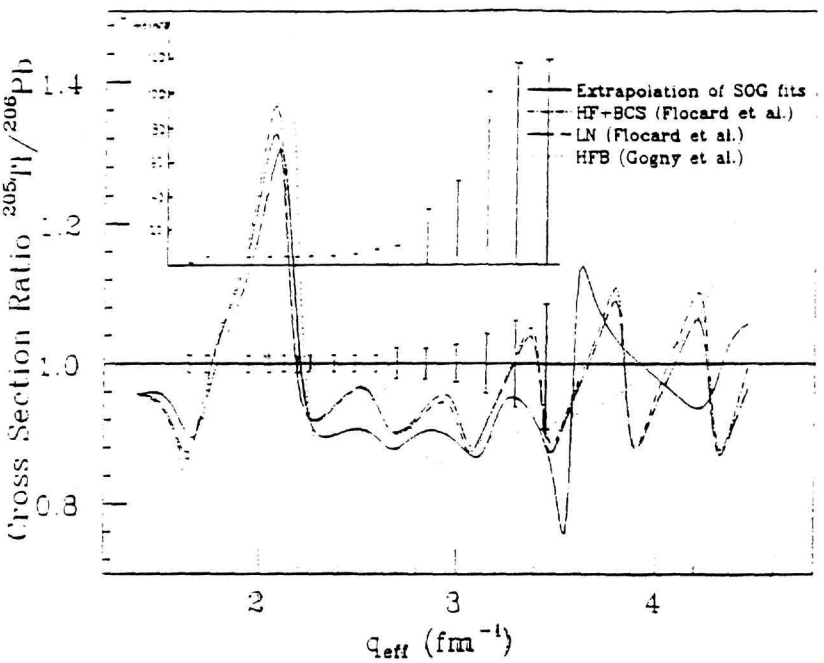

Fig.6 Running scenario for the experiment (see Table I). The bars on the horizontal line represent the statistical uncertainties of the measurements. The included diagram shows the time needed to complete each measurement. The curves show the results of various calculations for the $^{205}Tl/^{206}Pb$ elastic electron cross section ratio.

5.Summary

We have presented above the goals, the scope and the running scenario of an experiment that will be performed at the Bates Linear Accelerator Center. The experiment seeks to measure the differential elastic $^{208,207,206}Pb(e,e)$ and $^{205}Tl(e,e)$ cross sections in the broad range of momentum transfer 1.6 fm^{-1} < q < 3.4 fm^{-1}. Using the resulting data we shall study the influence of short-range correlations on the 3s proton orbital. We shall take into account the effect of core polarization on the measured cross sections and isolate it, in order to get clear information on

the nucleon correlations. Obtaining further guidance from results in atomic Fermi liquids, we shall study the effect of correlations on the 3s mean-field wave function by the study of their effect on the shape of this wave function.

References

[1] Frois B., Cavedon J. M., Goutte D., Huet M., Leconte P., Papanicolas C. N., Phan X. H., Platchkov S. K., Williamson S. E., Boeglin W. and Sick I. Nucl. Phys. **A396** (1983) 409

[2] Cavedon J. M., Frois B., Goutte D., Huet M., Leconte P., Papanicolas C. N., Phan X. H., Platchkov S. K., Williamson S. E., Boeglin W. and Sick I. Phys. Rev. Lett. **49** (1982) 978

[3] Cavedon J. M., Frois B., Goutte D., Huet M., Leconte P., Phan X. H., Platchkov S. K., Papanicolas C. N., Williamson S. E., Boeglin W. Sick I. and Heisenberg J. Phys. Rev. Lett. **58** (1987)195

[4] Papanicolas C. N. and Williamson S. E. Inst. Phys. Conf. Ser. No **105**

[5] Pandharipande V. R., Papanicolas C. N. and Wambach J. Phys.Rev. Lett. **53** (1984)1136

[6] Papanicolas C. N. 1985 in *Proc. IUCF Workshop on Nuclear Structure at High Spin, Excitation and Momentum Transfer*, Bloomington, edited by H. Nann, *AIP Conf. Proc.* 110, **142** (*American Institute of Physics*, New York, 1986)

[7] Experiment N° 9105 of the M.I.T., Middleton, Mass., USA

[8] Lewart D., Pandharipande V. R. and Pieper S. C. Phys. Rev. **B37** (1988) 4950

[9] Jaminon M., Mahaux C. and Ngo H. Nucl. Phys. **A240** (1985) 228

[10] Mahaux C. and Ngo H Nucl. Phys. **A431** (1984) 486

[11] B. Frois, J. B. Bellicard, J. M. Cavedon, M. Huet, P. Leconte, P. Ludeau, A. Nakada, Phan Zuan Ho and I. Sick Phys. Rev. Lett. (1976) **38** 152

[12] Friar J. L. and Negele J. W. Nucl. Phys. **A212** (1973) 93

[13] Sick I. Nucl. Phys. **A218** (1974) 509

[14] Dreher B., Friedrich J., Merle K., Rothaas H. and Luehrs G. Nucl. Phys. **A235** (1974) 219

[15] Bennour L., Heenen P. H., Bonche P., Dobaczewski J. and Flocard H. Phys. Rev. **C40** (1989) 2834

[16] Decharge J. and Gogny D. Phys. Rev. **C21** (1980) 1568